Some observations on the numerical solution of the Ottosen–Stenström–Ristinmaa high-cycle fatigue model

Osmo Kaleva[1] and Heikki Orelma

Summary   Some years ago, Ottosen, Stenström and Ristinmaa introduced a high-cycle fatigue model based on the continuum approach. The model is formulated as a fully implicit differential equation and an ordinary differential equation. The corresponding numerical solutions are compared. We demonstrate pitfalls in the process so that appliers are able to avoid these problems. Especially, we show that the results depend on the initial value of the evolution equation. We propose a method to choose such an initial value that the estimated Wöhler curve fits the measured data.

Introduction

The continuum approach to high-cycle fatigue modeling was first introduced by Ottosen *et al.* [9]. The idea was to define a so-called endurance surface in stress space. The location of the surface is governed by an evolution equation. The equation is a nonlinear, fully implicit differential equation, which is a special case of differential-algebraic equations (DAE). It follows that its numerical solution needs a dedicated methodology. Recently Lindström *et. al.* [8] formulated the Ottosen–Stenström–Ristinmaa model, or the OSR model for short, as an ordinary differential equation (ODE).

This paper is a part of our project concerning the OSR model. In [3], we studied the estimation of the model parameters. In [4], we discussed the statistical properties of the estimates obtained. Finally, in [5] we proposed a stochastic model for the stress process.

In this paper, we compare numerical solutions of the model formulated as a DAE and an ODE. We bring forward salient points, such as effects of the initial values, which have to be addressed, when solving the model.

---

[1]Corresponding author: osmo.kaleva@gmail.com

Evolution equation based continuum model

In this section, we briefly recall basic ideas of the evolution equation-based fatigue model as given in [9]. The fundamental idea is to define a so-called endurance surface $\beta(\boldsymbol{\sigma}, \boldsymbol{\alpha}) = 0$ in stress space, such that the damage develops when the stress $\boldsymbol{\sigma}$ is outside of the surface. As the authors did in [9], we use here a function of the form

$$\beta(\boldsymbol{\sigma}, \boldsymbol{\alpha}) = \frac{1}{\sigma_{-1}}(\overline{\sigma} + AI_1 - \sigma_{-1}), \tag{1}$$

where σ_{-1} and A are positive material parameters, $I_1 = \operatorname{tr}(\boldsymbol{\sigma})$ is the first stress invariant of $\boldsymbol{\sigma}$, and

$$\overline{\sigma} = \sqrt{\tfrac{3}{2}\operatorname{tr}((\boldsymbol{s} - \boldsymbol{\alpha})^2)}, \tag{2}$$

where $\boldsymbol{s} = \boldsymbol{\sigma} - \frac{1}{3}\operatorname{tr}(\boldsymbol{\sigma})\boldsymbol{I}$ and $\boldsymbol{I}$ stands for the identity matrix.

The variable $\boldsymbol{\alpha}$ denotes the center of the endurance surface, and it is governed by the evolution equation

$$\dot{\boldsymbol{\alpha}} = \begin{cases} C(\boldsymbol{s} - \boldsymbol{\alpha})\dot{\beta}, & \text{when } \beta, \dot{\beta} \geq 0, \\ 0, & \text{otherwise.} \end{cases} \tag{3}$$

The fundamental postulate of the continuum model is that the damage increases only if the stress state is outside the endurance surface and the endurance function β increases. The damage development is modeled by the damage equation

$$\dot{D} = \begin{cases} g(\beta, D)\dot{\beta}, & \text{if } \beta, \dot{\beta} \geq 0, \\ 0, & \text{otherwise,} \end{cases} \tag{4}$$

where g is an increasing damage rule function. Usually D is normalized such that at the beginning $D(0) = 0$ and the failure happens at the time t_f when $D(t_f) = 1$. In this paper, we choose the damage rule

$$g(\beta, D) = \frac{K}{(1 - D)^\gamma}e^{L\beta}.$$

This damage rule is called accumulated, since the damage history depends on the state of the damage.

Remark 1. *Recall that for symmetric matrices A, B $\operatorname{tr}(AB)$ defines an inner product. The corresponding norm $||\mathrm{A}||_{\mathrm{F}}^2 = \operatorname{tr}(A^2)$ is the Frobenius norm.*

Denote $r^2 = \frac{2}{3}(\sigma_{-1} - A\operatorname{tr}(\boldsymbol{\sigma}))^2$. Then the equation of the endurance surface $\beta(\boldsymbol{\sigma}, \boldsymbol{\alpha}) = 0$ may be written as $||\boldsymbol{s} - \boldsymbol{\alpha}||_{\mathrm{F}}^2 = r^2$.

In the principal stress space, the equation $\operatorname{tr}(\boldsymbol{\sigma}) = 0$ defines a deviatoric plane with a normal vector $\mathbf{n} = \begin{bmatrix} 1 & 1 & 1 \end{bmatrix}^T$. Since $\boldsymbol{s}$ and $\boldsymbol{\alpha}$ are deviatoric, they lie on the deviatoric plane and the endurance surface intersects the deviatoric plane along the circle $||\boldsymbol{s} - \boldsymbol{\alpha}||_{\mathrm{F}}^2 = \frac{2}{3}(\sigma_{-1})^2$. Figure 1 in [7] illustrates the situation.

Remark 2. *Recall that the damage rule of the OSR model is $g(\beta, D) = Ke^{L\beta}$. So the right-hand side does not contain the damage variable D. Now, if the damage rule is separable, i.e. $g(\beta, D) = g_1^{-1}(D)g_2(\beta)$, then a change of the damage variable yields the OSR type damage rule, cf. [6, 7, 8].*

In fact, let $G(D)$ be a primitive of $g_1(D)$, i.e. $G'(D) = g_1(D)$, and denote $D_1 = G(D)$. Substituting these equations into the damage evolution equation (4) gives us the OSR type damage evolution equation $\dot{D}_1 = g_2(\beta)\dot{\beta}$.

Note that in our case, the new damage variable D_1 contains the parameter γ, which has to be estimated alongside the other model parameters, cf. [3]. Finally $D = G^{-1}(D_1)$.

Evolution equation formulated as DAE

For the moment, we suppose that the stress history $\boldsymbol{\sigma}(t)$ is known. First, we have to estimate the parameters of the model as explained in [3, 9]. Then differentiating β, we obtain

$$\dot{\beta} = \frac{1}{\sigma_{-1}} \left(\sqrt{\tfrac{3}{2}} \, \frac{\operatorname{tr}((\boldsymbol{s} - \boldsymbol{\alpha})(\dot{\boldsymbol{s}} - \dot{\boldsymbol{\alpha}}))}{\sqrt{\operatorname{tr}((\boldsymbol{s} - \boldsymbol{\alpha})^2)}} + A\operatorname{tr}(\dot{\boldsymbol{\sigma}}) \right). \tag{5}$$

Let H denote the Heaviside function. Then we may write equation (3) as $0 = \dot{\boldsymbol{\alpha}} - C(\boldsymbol{s} - \boldsymbol{\alpha})\, \dot{\beta}\, H(\beta)H(\dot{\beta})$. Substituting equations (1) and (5) into the equation above, we obtain a fully implicit differential equation

$$0 = F(t, \boldsymbol{\alpha}(t), \dot{\boldsymbol{\alpha}}(t)), \; \boldsymbol{\alpha}(0) = \boldsymbol{\alpha}_0, \; \dot{\boldsymbol{\alpha}}(0) = \dot{\boldsymbol{\alpha}}_0. \tag{6}$$

Hence we have to solve a system of differential equations

$$\begin{cases} \dot{\boldsymbol{\alpha}} &= C(\boldsymbol{s} - \boldsymbol{\alpha})\, \dot{\beta}\, H(\beta)H(\dot{\beta}), \; \boldsymbol{\alpha}(0) = \boldsymbol{\alpha}_0, \; \dot{\boldsymbol{\alpha}}(0) = \dot{\boldsymbol{\alpha}}_0, \\ \dot{D} &= \frac{K}{(1-D)^\gamma} e^{L\beta}\, \dot{\beta}\, H(\beta)H(\dot{\beta}), \; D(0) = 0. \end{cases} \tag{7}$$

Proposition 3. *If $\beta(t, \boldsymbol{\alpha}(t)) \geq 0$ and $\dot{\beta}(t, \boldsymbol{\alpha}(t), \dot{\boldsymbol{\alpha}}(t)) \geq 0$ on some interval $I = [t_k, t_{k+1}]$, then*

$$-(1 - D(t_{k+1}))^{\gamma+1} + (1 - D(t_k))^{\gamma+1} = \frac{(\gamma+1)K}{L} \left(\exp(L\beta(t_{k+1})) - (\exp(L\beta(t_k))) \right).$$

Proof. The result follows when we integrate the damage equation

$$(1 - D)^\gamma \dot{D} = Ke^{L\beta}\dot{\beta},$$

from t_k to t_{k+1}. $\qquad \square$

Now suppose we have uniaxial case with a periodic stress history. Then, after a transient period, $\beta(t)$ stabilizes to a periodic state, cf. [9]. If $\gamma = 0$, then the increase of D is constant over the cycles. On one cycle we easily find intervals of increasing damage, *i.e.* intervals $[t_p, t_{p+1}]$, $p = 1, 3, 5, \cdots$, on which $\beta \geq 0$ and $\dot{\beta} \geq 0$. Hence by Proposition 3, we obtain ΔD during one cycle and consequently a lifetime N_f.

For the reader's convenience, we give a short description of a numerical method for solving a fully implicit differential equation (6). For more details, see [10] and the references therein. The most popular method is to use a backward differentiation formula of order k, BDFk. We start with the backward Euler method, which is BDF1. Note that also Holopainen *et al.* [2] used the backward Euler integration scheme with small time steps.

Now suppose we already have $\boldsymbol{\alpha}_n \approx \boldsymbol{\alpha}(t_n)$. We approximate

$$\dot{\boldsymbol{\alpha}}(t_{n+1}) \approx \tfrac{1}{h}(\boldsymbol{\alpha}_{n+1} - \boldsymbol{\alpha}_n),$$

which yields an equation for the next approximation $\boldsymbol{\alpha}_{n+1}$

$$0 = F(t_{n+1}, \boldsymbol{\alpha}_{n+1}, \tfrac{1}{h}(\boldsymbol{\alpha}_{n+1} - \boldsymbol{\alpha}_n)).$$

This equation is solved by iteration. The iterate $\boldsymbol{\alpha}_{n+1}^m$ is improved by

$$\boldsymbol{\delta} = \boldsymbol{\alpha}_{n+1}^{m+1} - \boldsymbol{\alpha}_{n+1}^m.$$

The linear approximation of F gives the equation

$$0 = F(t_{n+1}, \boldsymbol{\alpha}_{n+1}^m, \tfrac{1}{h}(\boldsymbol{\alpha}_{n+1}^m - \boldsymbol{\alpha}_n)) + M\boldsymbol{\delta}, \tag{8}$$

where the iteration matrix

$$M = F_{\boldsymbol{\alpha}}(t_{n+1}, \boldsymbol{\alpha}_{n+1}^m, \tfrac{1}{h}(\boldsymbol{\alpha}_{n+1}^m - \boldsymbol{\alpha}_n)) + \frac{1}{h} F_{\dot{\boldsymbol{\alpha}}}(t_{n+1}, \boldsymbol{\alpha}_{n+1}^m, \tfrac{1}{h}(\boldsymbol{\alpha}_{n+1}^m - \boldsymbol{\alpha}_n)).$$

Here $F_{\boldsymbol{\alpha}}$ and $F_{\dot{\boldsymbol{\alpha}}}$ denote the partial derivatives of F with respect to $\boldsymbol{\alpha}$ and $\dot{\boldsymbol{\alpha}}$. Solving this linear system of equations gives $\boldsymbol{\delta}$ and consequently $\boldsymbol{\alpha}_{n+1}^{m+1}$. Commonly used solvers use different details for solving equation (8).

Let $\dot{\beta}_{\boldsymbol{\alpha}}$ and $\dot{\beta}_{\dot{\boldsymbol{\alpha}}}$ denote the partial derivatives of $\dot{\beta}$ with respect to $\boldsymbol{\alpha}$ and $\dot{\boldsymbol{\alpha}}$. Then, by equation (3), we immediately obtain

$$F_{\boldsymbol{\alpha}}(t, \boldsymbol{\alpha}, \dot{\boldsymbol{\alpha}}) = \left(C\boldsymbol{I}\dot{\beta} - C(\boldsymbol{s} - \boldsymbol{\alpha})\, \dot{\beta}_{\boldsymbol{\alpha}} \right)\, H(\beta)\, H(\dot{\beta})$$

and

$$F_{\dot{\boldsymbol{\alpha}}}(t, \boldsymbol{\alpha}, \dot{\boldsymbol{\alpha}}) = \boldsymbol{I} - C(\boldsymbol{s} - \boldsymbol{\alpha})\, \dot{\beta}_{\dot{\boldsymbol{\alpha}}}\, H(\beta)\, H(\dot{\beta}).$$

What does a partial derivative with respect to a matrix mean? For example, take $\dot{\beta}_{\dot{\boldsymbol{\alpha}}}$. We propose to use the Gateaux derivative in the direction of the multiplicative unit element $\boldsymbol{I}$, $i.e.$

$$\dot{\beta}_{\dot{\boldsymbol{\alpha}}}(t, \boldsymbol{\alpha}, \dot{\boldsymbol{\alpha}}) = \lim_{u \to 0} \frac{\dot{\beta}(t, \boldsymbol{\alpha}, \dot{\boldsymbol{\alpha}} + u\boldsymbol{I}) - \dot{\beta}(t, \boldsymbol{\alpha}, \dot{\boldsymbol{\alpha}})}{u}.$$

With this choice we may apply formal differentiation rules for computing these partials. Furthermore, in one-dimensional case $\dot{\beta}_{\dot{\boldsymbol{\alpha}}}(t, \boldsymbol{\alpha}, \dot{\boldsymbol{\alpha}})$ reduces to the ordinary partial derivative.

A straightforward computation shows that the definition and application of formal differentiation rules give

$$\dot{\beta}_{\dot{\boldsymbol{\alpha}}}(t, \boldsymbol{\alpha}, \dot{\boldsymbol{\alpha}}) = -\frac{1}{\sigma_{-1}} \sqrt{\frac{3}{2}}\, \frac{\mathrm{tr}(\boldsymbol{s} - \boldsymbol{\alpha})}{\sqrt{\mathrm{tr}((\boldsymbol{s} - \boldsymbol{\alpha})^2)}}.$$

Similarly, a formal differentiation yields

$$\dot{\beta}_{\boldsymbol{\alpha}}(t, \boldsymbol{\alpha}, \dot{\boldsymbol{\alpha}}) = \frac{1}{\sigma_{-1}} \sqrt{\frac{3}{2}}\, \frac{\mathrm{tr}(\boldsymbol{s} - \boldsymbol{\alpha})\, \mathrm{tr}((\boldsymbol{s} - \boldsymbol{\alpha})(\dot{\boldsymbol{s}} - \dot{\boldsymbol{\alpha}})) - \mathrm{tr}(\dot{\boldsymbol{s}} - \dot{\boldsymbol{\alpha}})\, \mathrm{tr}((\boldsymbol{s} - \boldsymbol{\alpha})^2)}{(\mathrm{tr}((\boldsymbol{s} - \boldsymbol{\alpha})^2))^{\frac{3}{2}}}.$$

A more sophisticated method is to apply the BDFk formula. Now suppose that $t_{n+1} - t_n = h$ for all n and let $\boldsymbol{Q}(t)$ be the polynomial, which interpolates $\boldsymbol{\alpha}_{n+1-j}, j = 0, \cdots, k$. We demand that $\dot{\boldsymbol{\alpha}}_{n+1} = \boldsymbol{Q}'(t_{n+1})$. Using the Lagrange interpolation formula, Shampine [10] shows that

$$\dot{\boldsymbol{\alpha}}_{n+1} = \frac{1}{h} \sum_{j=0}^{k} a_j \boldsymbol{\alpha}_{n+1-j}.$$

Hence we have the iteration equation

$$0 = F\left(t_{n+1}, \boldsymbol{\alpha}_{n+1}, \tfrac{1}{h}\sum_{j=0}^{k} a_j \boldsymbol{\alpha}_{n+1-j}\right),$$

which is solved as above with the iteration matrix

$$M = F_{\boldsymbol{\alpha}} + \frac{a_0}{h} F_{\dot{\boldsymbol{\alpha}}}.$$

Some solvers also provide an option for computing consistent initial values, which in general is a difficult task.

Evolution equation formulated as ODE

Lindström *et al.* [8] recently introduced an auxiliary function

$$\nu(\boldsymbol{\sigma}, \dot{\boldsymbol{\sigma}}, \boldsymbol{\alpha}) = \frac{1}{\sigma_{-1} + C\sqrt{\frac{3}{2}\operatorname{tr}((\boldsymbol{s}-\boldsymbol{\alpha})^2)}}\left(\sqrt{\frac{3}{2}}\frac{\operatorname{tr}((\boldsymbol{s}-\boldsymbol{\alpha})\dot{\boldsymbol{s}})}{\operatorname{tr}((\boldsymbol{s}-\boldsymbol{\alpha})^2)} + A\operatorname{tr}(\dot{\boldsymbol{\sigma}})\right). \qquad (9)$$

They showed that $H(\beta)H(\dot{\beta})\dot{\beta} = H(\beta)H(\nu)\nu.$ and consequently that the OSR model (7) reduces to

$$\begin{cases} \dot{\boldsymbol{\alpha}} &= C(\boldsymbol{s}-\boldsymbol{\alpha})\ H(\beta)H(\nu)\nu,\ \boldsymbol{\alpha}(0) = \boldsymbol{\alpha}_0, \\ \dot{D} &= \frac{K}{(1-D)^{\gamma}}e^{L\beta}\ H(\beta)H(\nu)\nu,\ D(0) = 0, \end{cases} \qquad (10)$$

which is an ordinary differential equation. It follows that in the study of theoretical properties of the solution the well-developed theory of ordinary differential equations may be used. Furthermore for the numerical solution there are plenty of programs available in the public domain.

One-dimensional case

Now let σ be a uniaxial stress history and $\gamma = 0$, that is $\boldsymbol{\sigma} = \operatorname{diag}(\sigma, 0, 0)$ with deviatoric matrices $\boldsymbol{s} = \operatorname{diag}(\frac{2}{3}\sigma, -\frac{1}{3}\sigma, -\frac{1}{3}\sigma)$ and $\boldsymbol{\alpha} = \operatorname{diag}(\alpha, -\frac{1}{2}\alpha, -\frac{1}{2}\alpha)$. A straightforward computation gives $\beta = \frac{1}{\sigma_{-1}}(|\sigma - \frac{3}{2}\alpha| + A\sigma - \sigma_{-1})$ and hence

$$\dot{\beta} = \frac{1}{\sigma_{-1}}(\operatorname{sgn}(\sigma - \tfrac{3}{2}\alpha)(\dot{\sigma} - \tfrac{3}{2}\dot{\alpha}) + A\dot{\sigma}).$$

Here sgn denotes the signum function and $\operatorname{diag}(a, b, c)$ a diagonal matrix with diagonal elements as arguments. Similarly we get

$$\nu = \frac{\left(\operatorname{sgn}(\sigma - \tfrac{3}{2}\alpha) + A\right)\dot{\sigma}}{\sigma_{-1} + C|\sigma - \tfrac{3}{2}\alpha|}.$$

Experimental datasets

We will demonstrate the behavior of the model with three different datasets. Measurements of alloy steel SAE 4340 were adopted from [9]. Experimental values of lifetimes of S45C carbon steel were given in [11]. Lindström *et al.* [8] provided model parameter

estimates for 7050-T7451 aluminum alloy. In Table 1, we give model parameter estimates for all these datasets.

Material	A	σ_{-1}	C	K	L
NiCrMo alloy steel SAE 4340	0.2250	490	0.8083	6.9668e-06	18.4562
Aluminum alloy 7050-T7451	0.2611	113.3	0.5039	5.111e-06	2.556
Carbon steel S45C	0.2559	220	0.5000	10.511e-06	0.1000

Table 1. Parameters of the OSR model for some materials

Computational details and results

In this section, we compare the DAE and ODE solutions of the model with the datasets given above, and we especially demonstrate the dependence of the solution on the initial value α_0.

In the examples, we apply a stress history $\sigma(t) = \sigma_m + \sigma_a \sin(t)$. Since it has a period of 2π, we integrate over intervals $[2k\pi, 2(k + 1)\pi]$, $k = 0, 1, \cdots$, with time step $\Delta t = 0.001$. During the process we check the convergence of β. The convergence criterion is the maximum difference of β in two consecutive intervals. The convergence tolerance depends on the problem as well as on the solution method. We found out that generally with DAE-solver it was possible to use more strict tolerances. The lifetime for each initial value is obtained as described above. We report only the maximum lifetime.

In the numerical computations, we use differential equation solvers *ode15i* and *ode45* as implemented in Matlab. Ode15i solves fully implicit differential equations. It is a variable-step, variable-order solver based on the BDFk of orders $k = 1, \cdots, 5$. Note, that for ode15i we also need an initial value $\dot{\boldsymbol{\alpha}}_0$. The initial values must be consistent, meaning that $F(0, \boldsymbol{\alpha}_0, \dot{\boldsymbol{\alpha}}_0) = 0$. The Matlab function *decic* computes consistent initial values. For more information, see [10]. Ode45 solves nonstiff differential equations. It is based on an explicit Runge–Kutta (4,5) formula as given in [1].

First we analyze dataset S45C. The results are given in Figures 1–4.
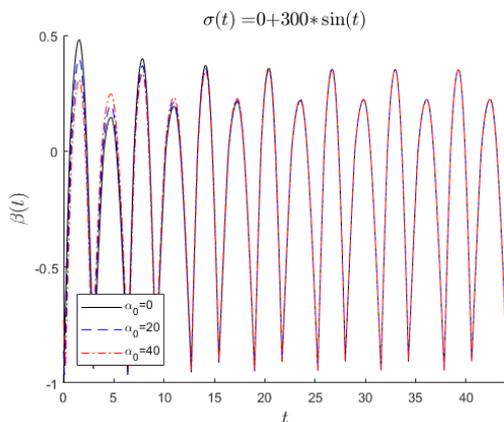
Figure 1. Endurance function, DAE solution, dataset S45C
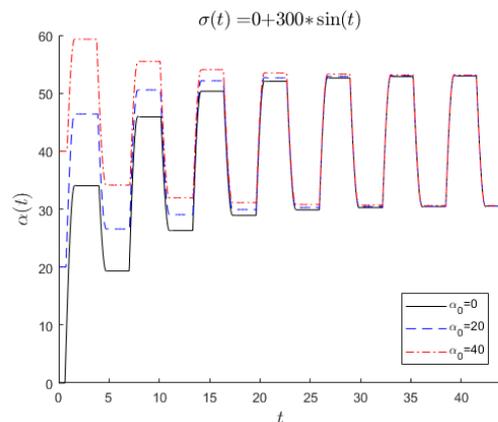
Figure 2. Back-stress α; maximum lifetime $N_f = 163462$ with $\alpha_0 = 40$ MPa

6
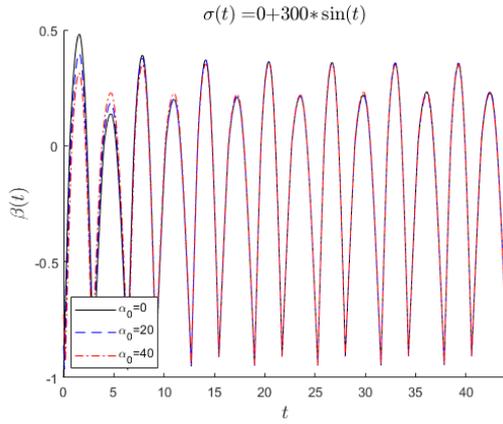
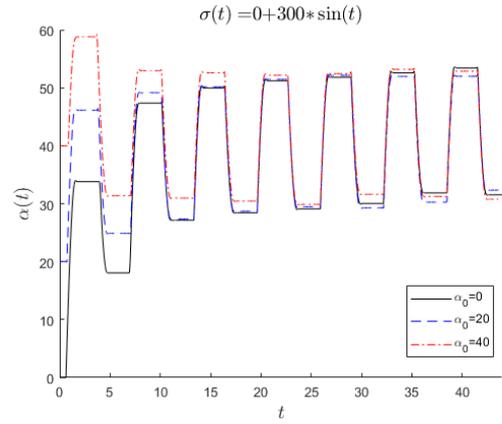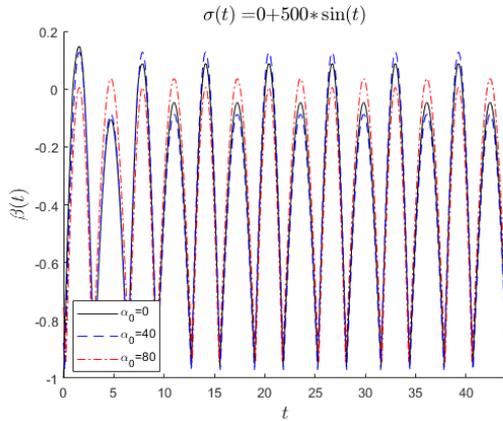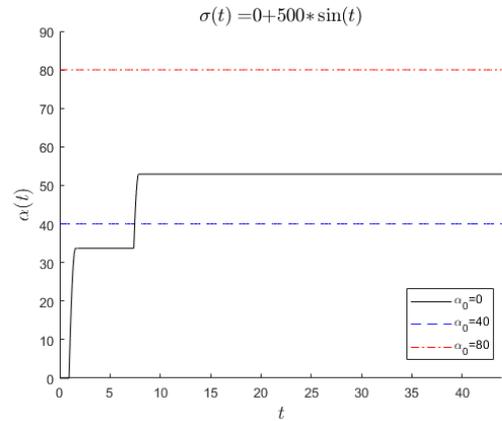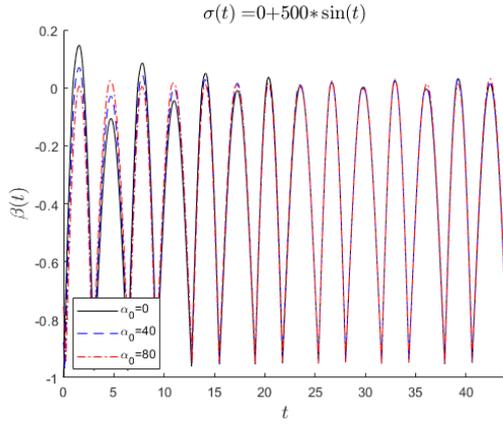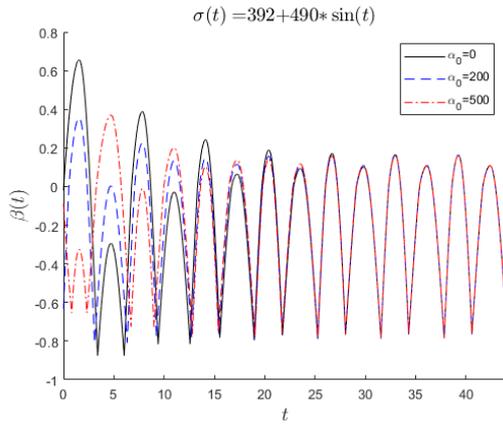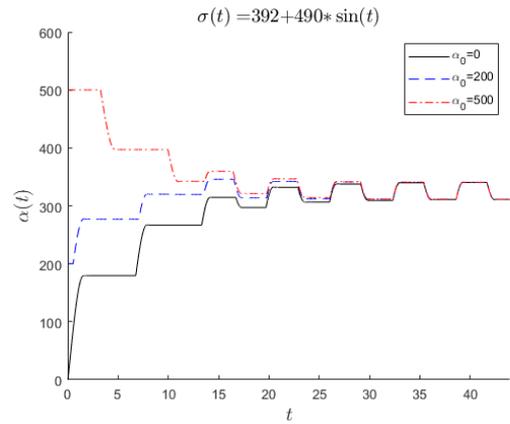Figure 3. Endurance function, ODE solution, dataset S45C

Figure 4. Back-stress α; maximum lifetime $N_f = 162662$ with $\alpha_0 = 40$ MPa

We see that both solutions behave as expected. After a transient, the back-stress and the evolution function stabilize into a cyclic steady-state, which is the same for all initial values. It follows that also lifetimes are equal for all initial values. Furthermore, the lifetimes given by the DAE and ODE solutions are approximately the same.

Next we take dataset SAE 4340. Now the DAE solution behaves oddly. Back-stresses stabilize to different constant values and the steady-state of β depends on the initial value. In the ODE solution, there seems to be no cyclic steady-state for back-stress. However the steady-state of β is essentially the same for all initial values. The lifetimes of these solutions are incompatible. Figures 5–8 present the results.

Figure 5. Endurance function, DAE solution, dataset SAE 4340

Figure 6. Back-stress α; maximum lifetime $N_f = 2567297$ with $\alpha_0 = 80$ MPa

7

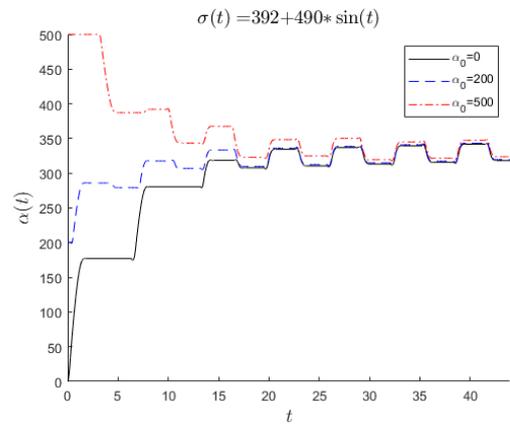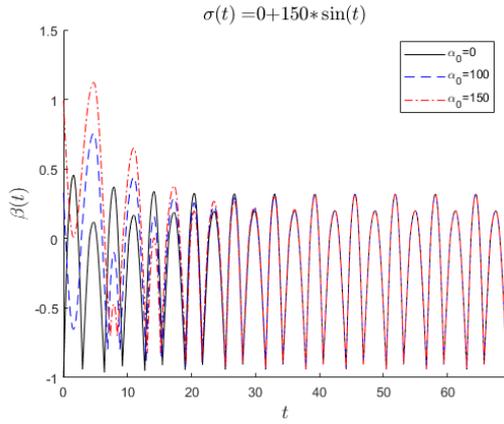Figure 7.   Endurance function, ODE solution, dataset SAE 4340
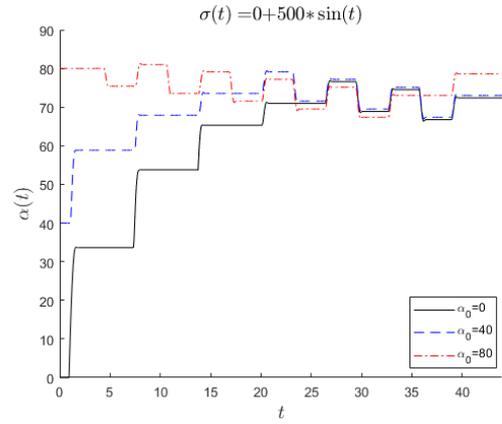
Figure 8.   Back-stress α; maximum lifetime $N_f = 6170373$ with $\alpha_0 = 40$ MPa

Now, instead of $\sigma_m = 0$, we apply a positive mean stress. With a stress function $\sigma(t) = 0.8\,\sigma_{-1} + \sigma_{-1}\sin(t)$, both solutions behave similarly according to the theory, and the lifetimes are of the same magnitude. This is seen in Figures 9–12.

Figure 9.   Endurance function, DAE solution, dataset SAE 4340

Figure 10.   Back-stress α; maximum lifetime $N_f = 105309$ with $\alpha_0 = 200$ MPa
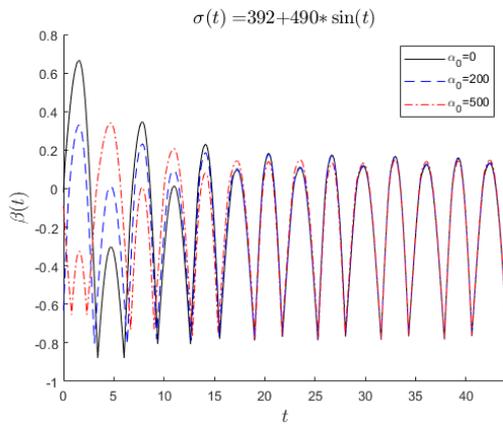
Figure 11.   Endurance function, ODE solution, dataset SAE 4340

Figure 12.   Back-stress α; maximum lifetime $N_f = 97850$ with $\alpha_0 = 500$ MPa

Finally, in Figures 13–16 we see that in dataset 7050-T7451, both solutions give similar results, which are consistent with theoretical expectations.

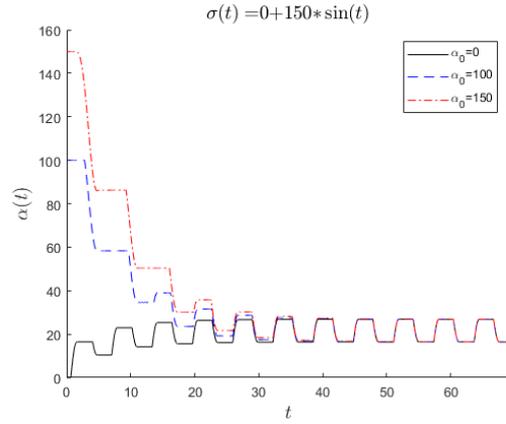Figure 13. Endurance function, DAE solution, dataset 7040-T7451

Figure 14. Back-stress α; maximum lifetime $N_f = 260777$ with $\alpha_0 = 150$ MPa
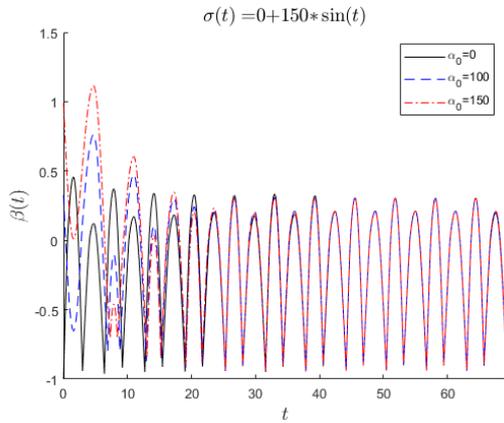

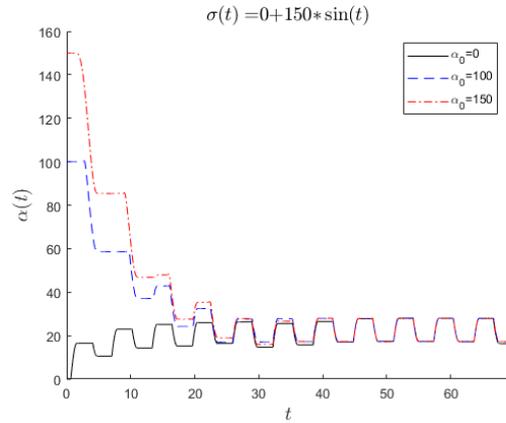Figure 15. Endurance function, ODE solution, dataset 7040-T7451

Figure 16. Back-stress α; maximum lifetime $N_f = 272618$ with $\alpha_0 = 0$ MPa

Wöhler curve estimation

As we have seen, the estimated lifetime for a material depends on the solution method and initial values. For the DAE solution, this is demonstrated in Figures 17 and 18.
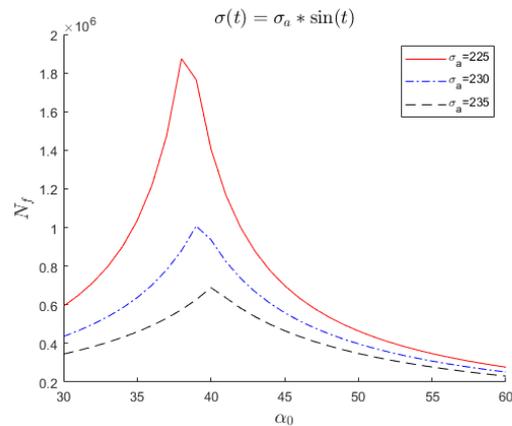

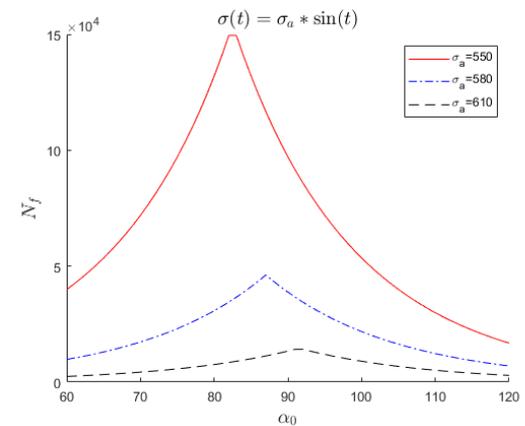Figure 17. Lifetime dependence on initial value, dataset S45C

Figure 18. Lifetime dependence on initial value, dataset SAE 4340

9

Remark 4. *If the differential system is well-behaved, then in Figures 17 and 18 the lifetimes should be constant, at least locally. On the other hand, if the system is chaotic, then the lifetimes probably vary randomly. However, we see that the dependence of the lifetime on the initial value is a smooth curve.*

One reason may be the discontinuous Heaviside function in the model.

So, how should we select an appropriate initial value for the back-stress? We choose the initial value, which gives the maximal lifetime. With this choice the model produces lifetimes compatible with experimental data.

In the Wöhler curve computations, we applied a grid of initial values, and the greatest of lifetimes obtained was accepted. We observed that sometimes a differential equation solver fails to integrate over an interval. It follows that we have to tinker with the input parameters of the programs even to get a result.

Figure 19 illustrates the Wöhler curve estimate for SAE 4340. The curves are identical at small amplitudes. However, the ODE solution behaves strangely at high amplitudes. We ran the models until both solutions reached a stable state for all amplitudes and initial values. For this we had to apply a loose convergence tolerance $tol = 5 \cdot 10^{-1}$. The computation with the exhaustive search of initial values took 63 seconds with DAE and 106 seconds with ODE.

Next we ran the models with an optimal initial value as given by the equation (11). We hoped that we could tighten the convergence criteria. This was not the case and we applied tolerance $tol = 5 \cdot 10^{-1}$. The computation took only 4 seconds with DAE and 6 seconds with ODE. Again the ODE solution behaves strangely as seen in Figure 20. Now the curve was even worse than in Figure 19.
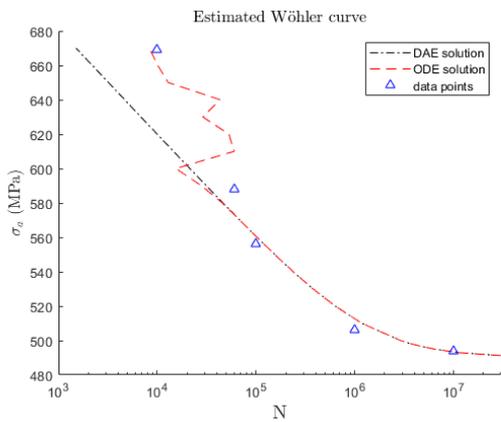

Figure 19.   Estimated Wöhler curve with exhaustive search
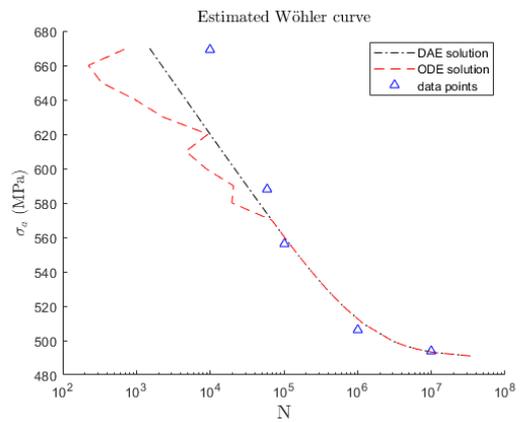
Figure 20.   Estimated Wöhler curve with optimal initial value

We observed that generally the DAE solution stabilized more rapidly than the ODE solution. Also with DAE it was possible to use tighter tolerances. However, we have no explanation for the strange behavior of the ODE solution.

The DAE model fits well to four data points. Instead one data point falls away from the model. We estimated the model parameters using all 20 data points given in [9]. Only 5 of them, which appear in Figures 19 and 20, were measured with mean stress $\sigma_m = 0$. This may explain the discrepancy.

Obtaining a good initial value

We have seen that different initial values give distinct lifetimes. Furthermore, the exhaustive search for a good initial value was time consuming. In this section, we address the question, whether it is possible to choose a good initial value beforehand.

For the DAE model, we selected a representative set of amplitudes and computed initial values α_{opt}, which gave the maximum lifetime. We found out that α_{opt} depends linearly on the amplitude σ_a. Next, we fitted a straight line to the computed data. Hence the optimal initial value curve is

$$\alpha_{opt} = c_1 \sigma_a + c_2, \tag{11}$$

where c_1 and c_2 are material parameters.

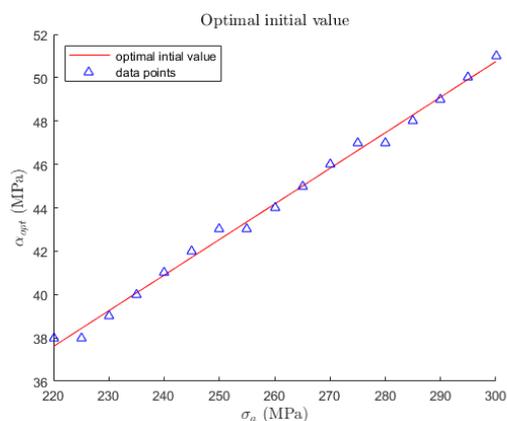The situation is illustrated in Figures 21 and 22.

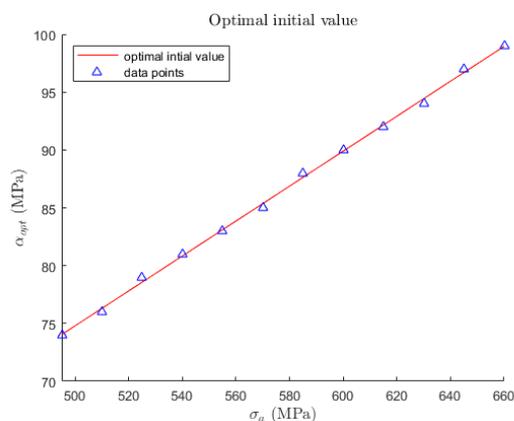Figure 21.   The optimal initial value curve, dataset S45C

Figure 22.   The optimal initial value curve, dataset SAE 4340

In Table 2, we give the parameters of the optimal initial value curve for the three material discussed in this paper.

Material	c_1	c_2 (MPa)
NiCrMo alloy steel SAE 4340	0.1510	-0.7308
Aluminum alloy 7050-T7451	0.1667	1.1667
Carbon steel S45C	0.1642	1.4804

Table 2. Parameters of the initial value curve for some materials

Remark 5. *In [7], Lindström characterized the back-stress as follows:* We can understand the presence of a back-stress as inelastic deformation associated with microdamage in individual grains or grain boundary segments.

With the optimal choice of the initial value we try to put α_0 directly into the interval, where back-stress varies after the transient phase.

Conclusions

We have experimentally compared the DAE and ODE solutions for the OSR model with uniaxial examples. The dependence on initial values were discussed. For the Wöhler curve estimation, we suggest the following procedure: use the DAE formulation and compute an initial value by Equation (11), if available. Otherwise, apply a grid of initial values and accept the greatest of lifetimes obtained.

References

[1] J. R. Dormand and P. J. Prince, A family of embedded Runge–Kutta formulae, *Journal of Computational and Applied Mathematics* 6 (1980) 19–26.

[2] S. Holopainen, R. Kouhia and T. Saksala, Continuum approach for modelling transversely isotropic high-cycle fatigue, *European Journal of Mechanics A/Solids* 60 (2016) 183–195.

[3] O. Kaleva, H. Orelma and D. Pethukov, Parameter estimation of a high-cycle fatigue model combining the Ottosen–Stenström–Ristinmaa approach and Lemaitre–Chaboche damage rule, *International Journal of Fatigue*, 147 (2021), https://doi.org/10.1016/j.ijfatigue.2021.106153.

[4] O. Kaleva and H. Orelma, Statistical properties of the model parameters in the continuum approach to high-cycle fatigue, *Probabilistic Engineering Mechanics*, 63 (2021), https://doi.org/10.1016/j.probengmech.2021.103117.

[5] O. Kaleva and H. Orelma, Modeling stress history as a stochastic process, *International Journal of Fatigue*, 143 (2021), https://doi.org/10.1016/j.ijfatigue.2020.105996.

[6] J. Lemaitre and J. L. Chaboche, *Mechanics of Solid Materials*, Cambridge University Press, 1990.

[7] S. B. Lindström, Continuous-time, high-cycle fatigue model for nonproportional stress with validation for 7075-T6 aluminum alloy, *International Journal of Fatigue*, 140 (2020), https://doi.org/10.1016/j.ijfatigue.2020.105839.

[8] S. B. Lindström, C. Thore, S. Suresh and A. Klarbring, Continuous-time, high-cycle fatigue model: Validity range and computational acceleration for cyclic stress, *International Journal of Fatigue*, 136 (2020), https://doi.org/10.1016/j.ijfatigue.2020.105582.

[9] N. Ottosen, R. Stenström and M. Ristinmaa, Continuum approach to high-cycle fatigue modeling, *International Journal of Fatigue*, 30 (6) (2008) 996–1006, https://doi.org/10.1016/j.ijfatigue.2007.08.009.

[10] L. F. Shampine, Solving $0 = f(t, y(t), y'(t))$ in Matlab, *Journal of Numerical Mathematics* 10 (4) (2002) 291–310.

[11] K. Shiozawa and N. Z. Gakkai, *Databook on fatigue strength of metallic materials, vol 1*, Elsevier, 1996.

Osmo Kaleva, Heikki Orelma
Tampere University
osmo.kaleva@gmail.com, heikki.orelma@tuni.fi